Durability of solid oxide fuel cells using sulfur containing fuels

Anke Hagen*, Jens F.B. Rasmussen, Karl Thydén

Risoe DTU, Fuel Cells and Solid State Chemistry Division, Frederiksborgvej 399, DK 4000 Roskilde, Denmark

ARTICLE INFO

ABSTRACT

The usability of hydrogen and also carbon containing fuels is one of the important advantages of solid oxide fuel cells (SOFCs), which opens the possibility to use fuels derived from conventional sources such as natural gas and from renewable sources such as biogas. Impurities like sulfur compounds are critical in this respect. State-of-the-art Ni/YSZ SOFC anodes suffer from being rather sensitive towards sulfur impurities. In the current study, anode supported SOFCs with Ni/YSZ or Ni/ScYSZ anodes were exposed to H$_2$S in the ppm range both for short periods of 24 h and for a few hundred hours. In a fuel containing significant shares of methane, the reforming activities of the Ni/YSZ and Ni/ScYSZ anodes were severely poisoned already at low H$_2$S concentrations of ∼2 ppm H$_2$S. The poisoning effect on the cell voltage was reversible only to a certain degree after exposure of 500 h in the state-of-the-art cell, due to a loss of percolation of Ni particles in the Ni/YSZ anode layers closest to the electrolyte. Using SOFCs with Ni/ScYSZ anodes improved the H$_2$S tolerance considerably, even at larger H$_2$S concentrations of 10 and 20 ppm over a few hundred hours.

© 2011 Elsevier B.V. All rights reserved.

1. Introduction

The usability of not only hydrogen but also carbon containing fuels is one of the important advantages of solid oxide fuel cells (SOFCs), which opens the possibility to use fuels derived from conventional sources such as natural gas and from renewable sources such as biogas or gasification gas as well. Therefore, these fuels have been studied comprehensively with respect to performance and durability of state-of-the-art SOFCs as for example by Yokokawa et al. [1] and Hagen et al. [2].

Approaching more realistic fuels, also minor and trace components have to be included in the studies as well. Sulfur compounds have attracted special attention as they are contained in biogas and gasification gas, but also in diesel CPO (catalytic partial oxidation) gas, while reformate usually has been through a thorough desulfurization prior to the reforming and the obtained fuel thus can be considered sulfur free when entering the SOFC. State-of-the-art Ni/YSZ SOFC anodes posses a high activity for reforming of methane. However, as conventional reforming catalysts also these anodes suffer from being rather sensitive towards sulfur impurities [3–10]. A considerable number of these studies were carried out on model systems, electrolyte supported cells and/or lower methane concentrations in the fuel. Comprehensive, detailed studies on long-term effects of relevant sulfur impurity concentrations in fuel mixtures containing larger amounts

of methane on technological (anode supported) SOFCs are still sparse.

Both, the effect of sulfur impurities on the reforming activity and the electrochemical reaction have been studied. It was found that the reforming activity was poisoned to a larger degree and that there are different active sites in the Ni/YSZ anode for either reforming or electrochemical reaction, when comparing anode supported cells at 850 °C and poisoning periods of 24 h in hydrogen and methane containing fuel [6,10]. The same conclusion was drawn by Rostrup-Nielsen et al. [8], after studying a 5 cell SOFC stack exposed to a fuel containing 1.5 vol% CH$_4$ (rest H$_2$, CO, CO$_2$, N$_2$) and H$_2$S in the ppm range. In order to improve the sulfur tolerance of SOFC anodes, attempts to modify the Ni/YSZ system and to develop new anodes as well have been reported in the literature [5,11,12].

In the present study, technological, anode supported SOFCs with the compositions LSM/YSZ–YSZ–Ni/YSZ or LSM/YSZ–ScYSZ–Ni/ScYSZ for cathode/electrolyte/anode, both series manufactured using typical scalable processes, have been studied for their performance and durability in a fuel containing the significant share of methane of 29% in the presence of H$_2$S at 850 °C. Steam was added to the fuel to allow for the steam reforming of the methane. A steam to carbon ratio of two was applied to avoid coke formation. The cells were exposed to H$_2$S in the ppm range both for short periods of 24 h and for longer periods up to 500 h. Poisoning of the reforming reaction on Ni/YSZ vs. Ni/ScYSZ SOFCs was investigated. The study also included the effect of current load vs. open circuit voltage (OCV) and H$_2$S concentrations in the fuel. Furthermore, a thorough micro-structural analysis of selected tested cells was carried out.

* Corresponding author. Tel.: +45 4677 5884; fax: +45 4677 5858.
  E-mail address: anke@risoe.dtu.dk (A. Hagen).

2. Experiments

Anode supported SOFCs with Ni/YSZ anodes, YSZ electrolytes, and LSM/YSZ cathodes were used for testing (denoted as *Ni,YSZ,LSM*). The active area was 4 cm × 4 cm. The Ni/YSZ anode support was tape-casted, while Ni/YSZ anode, YSZ electrolyte, and LSM/YSZ cathode were sprayed. More details about cell manufacture and performance are given in [13]. A second series of cells was manufactured with Sc doped YSZ in the anode and electrolyte layers (denoted as *Ni,ScYSZ,LSM*). In these cells, Ni/YSZ anode support, Ni/Sc-YSZ anode, and Sc-YSZ electrolyte were tape-casted and the LSM/YSZ cathode was screen-printed [14].

Electrochemical tests were performed in a sealed setup comprising alumina test-houses with current and voltage probes, temperature probes and pO_2 sensors. Gold and nickel foil current collectors were used at the cathode and anode side, respectively. LSM and Ni/YSZ gas distribution components were used at the cathode and anode side, respectively (for details see [15]). The cells were sealed and reduced at 1000 °C and afterwards the temperature was decreased to 850 °C.

The initial performance of the cells was characterized by a fingerprint comprising of iV curves and impedance spectra (oscillating current of approximately 60 mA, 0.08 Hz–82 kHz, Solartron SI 1260 impedance analyser,) at 750 and 850 °C. Air was used as cathode gas (140 l h^{-1}) and hydrogen (24 l h^{-1}) with 4 or 20% water vapor was applied on the anode side. The same procedure was repeated after completion of the testing.

For further (aging) testing the fuel gases (H_2, CH_4 and O_2) were supplied through mass flow controllers. H_2 and O_2 ($pH_2 > pO_2$) were mixed to form a H_2/H_2O gas mixture of the desired composition. H_2 could be further moisturized in a water bottle (~4% H_2O). H_2S from a pressurized H_2S/H_2-bottle containing 218 ppm H_2S was mixed with CH_4 through mass flow controllers. The thus obtained two mixtures were combined and led into the cell test house. The total fuel flow at the cell inlet was kept constant at 10 l h^{-1}. Air was used on the cathode side (140 l h^{-1}). The SOFC performance was evaluated by measuring the cell voltage, the in-plane voltage in anode and cathode as well as by impedance spectroscopy. The fuel composition at the in- and outlet of the cell was measured by using pO_2 sensors. Specifically, the voltage between air (supplied to the sensor) and the fuel was measured and the corresponding fuel composition calculated using Nernst's law.

Polished cross sections of selected cells were analyzed by scanning electron microscopy (SEM) after testing, in a Supra 35 from Carl Zeiss, using the low-voltage charge contrast technique described by Thydén et al. [16]. This technique enables visualization of the percolating electrically conducting phase in the electrodes, Ni particles in this work.

3. Results and discussion

3.1. Effect of H_2S on the reforming activity of the anodes in Ni,YSZ,LSM and Ni,ScYSZ,LSM SOFCs.

The aim was to study the effect of H_2S on the methane reforming reaction both on SOFCs with Ni/YSZ (state-of-the-art) and Ni/ScYSZ anodes by adding H_2S at 850 °C. These studies were performed at OCV and thus the pure catalytic effect was probed. A methane containing fuel of the following composition was used: 13% H_2, 29% CH_4, 58% H_2O. H_2S concentrations from 2 to 24 ppm were added for periods of 24 h. By means of pO_2 sensors, the fuel composition was measured at the fuel inlet position (pO_2-in) and the fuel outlet position (pO_2-out).

As the measured steady state values for the cell voltage (OCV), like the values for pO_2-in and pO_2-out, can be related to specific gas
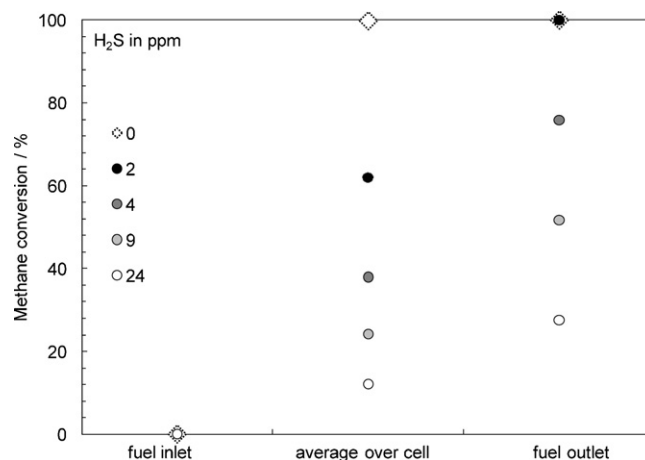

Fig. 1. Methane conversion ((CH_4inlet-CH_4)/CH_4inlet in %) calculated from measured voltages at the inlet (pO_2-in), over the cell (OCV), and outlet (pO_2-out) of the Ni,YSZ,LSM cell as function of H_2S concentration in a 13% H_2, 58%, H_2O 29% CH_4 fuel at OCV and 850 °C. The methane conversion will be unevenly distributed over the cells anode area (increasing with progressing distance from fuel inlet), but that would require more local sensors and was not measured here.

compositions, a profile of the gas composition can be established at these positions in the testing setup, i.e. the fuel inlet, the cell (the measured OCV gives an average over the whole cell area) and the fuel outlet. This approach can be illustrated by the following examples: In case of OCV and a hydrogen fuel free of H_2S, the gas composition that is entering and leaving the cell is the same and thus the measured voltages (cell voltage, pO_2-in and pO_2-out) are the same. If a methane plus steam containing fuel is entering the cell, the pO_2-in would show a voltage corresponding to this composition, whereas the cell voltage would be higher, as the methane is converted when passing over the Ni containing anode of the SOFC. pO_2-out would normally correspond to a fuel mixture, where all methane is converted.

When the methane conversion by steam reforming is complete, the gas composition corresponds to equilibrium values at 850 °C, yielding a theoretical voltage of 995 mV. The lower the methane conversion the lower is the voltage. At zero methane conversion, the theoretical voltage is 852 mV. In Table 1, the gas compositions for these two cases are listed. Knowing the voltage values, the methane conversion can be calculated.

In Fig. 1 the methane conversions calculated from the measured voltages at the fuel inlet, the cell voltage and the fuel outlet are plotted for different H_2S concentrations in the fuel for a Ni,YSZ,LSM SOFC.

According to the measured pO_2-in, the fuel gas entering the cell corresponds to the feed composition at zero ppm H_2S. This underlines the fact that mere heating of methane and steam to 850 °C is not sufficient but that a catalyst is necessary for the methane reforming reaction. As soon as the fuel has made contact with the anode of the SOFC, methane is converted under the conditions used in this test (temperature and flow). From the measurements it cannot be concluded at which point of the cell's anode area the conversion has been completed, however, it can be expected, that the methane conversion was already 100% shortly after the fuel inlet. Addition of only 2 ppm H_2S lead to a decrease of the methane conversion over the cell, as the expected theoretical value of 995 mV was not obtained. According to Fig. 1, the reforming reaction is progressing over the cell (and thus anode) area from fuel inlet (no conversion) to the outlet, where the methane conversion has reached 100% at 2 ppm H_2S. When increasing the H_2S concentration to 4 ppm and further on, the methane conversion was decreasing more and the whole anode area was not sufficient to achieve full

Table 1
Calculated gas compositions and voltages at 850 °C for complete and zero methane conversion using a gas mixture containing 13% H_2, 29% CH_4, 58% H_2O.

Methane conversion (%)	CH_4 (%)	CO (%)	CO_2 (%)	H_2 (%)	H_2O (%)	Voltage (mV)
100	0	15	3	66	16	995
0	29	0	0	13	58	852

conversion. No line was drawn between the measured points as the trend cannot be deduced from these few values.

The poisoning effect can also be evaluated by following the cell voltage continuously under H_2S exposure. This approach is usually used in the related literature such as [7,17,18]. When starting the H_2S exposure at OCV, the cell voltage dropped sharply and reached afterwards a constant level. In Fig. 2 this cell voltage drop (ΔV) and the corresponding calculated methane conversion is plotted as function of the H_2S concentration. The obtained trend was not linear; at concentrations of ~20 ppm, the cell voltage drops seem to achieve a constant level on both SOFC types when increasing the H_2S concentration further. Although the cell voltage drops on the Ni,ScYSZ,LSM cell were slightly smaller and thus the methane conversion slightly larger over the whole H_2S concentration range, a significant difference between the cells with the two different anodes (and electrolytes) was not observed.

The magnitude of the cell voltage drop on the Ni,YSZ,LSM cell was earlier related to the poisoning of the reforming activity, i.e. it corresponds to a decrease of the fraction of methane converted via steam reforming [10]. In other words, the methane concentration in the fuel gas increased from close to zero at 0 ppm H_2S (nearly complete reforming on the SOFC anode) to ~20% at 24 ppm H_2S (poisoning of the reforming, see also discussion above).

It can only be speculated at this point, if the slightly smaller poisoning effect of H_2S on the reforming activity of the Ni,ScYZ,LSM cell was due to a slightly different Ni particle size distribution in this anode or an actual result of the presence of Sc. It has been observed that the Ni particle size distributions of the Ni,YSZ,LSM and Ni,ScYSZ,LSM cells are not exactly the same, although a complete quantitative analysis is not yet available. Eguchi et al. [19] have studied the reforming activity of Ni–ScYSZ vs. Ni–YSZ materials by using powder mixtures. It was concluded the Ni particle size distribution had a significant effect on the reforming activity, while the presence of Sc actually slightly decreased it. This result points to the importance of the structure and the Ni particle size
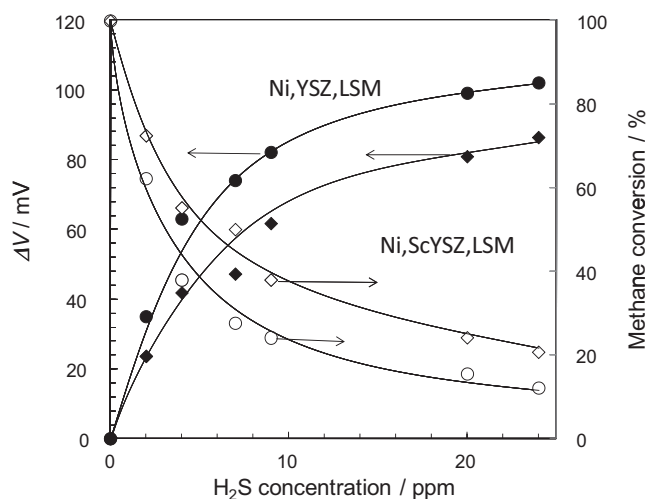
distribution of the two different anodes for the reforming activity and the lesser importance of the presence of Sc.

The tests at OCV suggest for the first time for full, anode supported SOFCs that the reforming activity at 850 °C is poisoned to a similar extent on both Ni,YSZ,LSM and Ni,ScYSZ,LSM SOFCs used here.

3.2. Effect of H_2S on the long-term durability of Ni,YSZ,LSM and Ni,ScYSZ,LSM SOFCs

In further test series, the H_2S exposure was prolonged to 500 h at 850 °C and a current load of 1 A cm^{-2} was applied. Previous studies have shown that a Ni,YSZ,LSM SOFC did not show significant degradation under these conditions in a $H_2/CO/H_2O$ fuel in the absence of H_2S [2,6]. In Fig. 3, the cell voltage trends are shown as function of the operating time.

The Ni,YSZ,LSM cell showed already a small degradation in the range of 10% before starting the H_2S exposure. The cell voltage dropped by ~70 mV when H_2S was started. This drop was larger than the one under OCV when the same 2 ppm H_2S were added to the fuel (35 mV, see Fig. 2). Under exposure of 2 ppm H_2S, the cell voltage experienced a severe degradation of 237 mV kh^{-1} (40%). After 500 h, the H_2S addition was stopped, where after the cell voltage increased immediately to a level lower than the initial one before the period under H_2S.

The cell voltage behavior was different when testing the Ni,ScYSZ,LSM cell. First, the cell voltage did not decrease during the initial period in the methane containing fuel. The cell voltage dropped rapidly by ~50 mV, when the H_2S was started. Under H_2S, the cell voltage decreased over time, but not with a constant rate. The degradation rate decreased with operating time. While it was 120 mV kh^{-1} (14%) calculated from the first 48 h operating under H_2S, it dropped to zero mV kh^{-1} when considering the last 300 h.

The cell voltage drops observed when starting the H_2S exposure are an indication of the covering of the active sites (both for reforming of methane and the electrochemical reaction) by H_2S. It has been speculated, if current has an effect on the sulfur coverage. Supply of oxygen ions through the electrolyte might facilitate desorption of
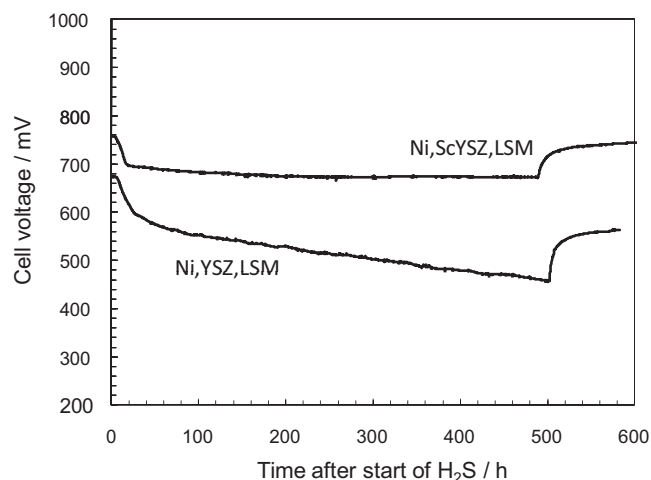

Fig. 2. Cell voltage drops (ΔV in mV, black symbols) and the corresponding calculated methane conversions (open symbols) as function of H_2S concentration in a 13% H_2, 58%, H_2O 29% CH_4 fuel at OCV and 850 °C for the Ni,YSZ,LSM (circles) and Ni,ScYSZ,LSM (rhombs) cells.

Fig. 3. Cell voltage under 2 ppm H_2S in a 13% H_2, 58%, H_2O 29% CH_4 fuel at 850 °C, 1 A cm^{-2}.
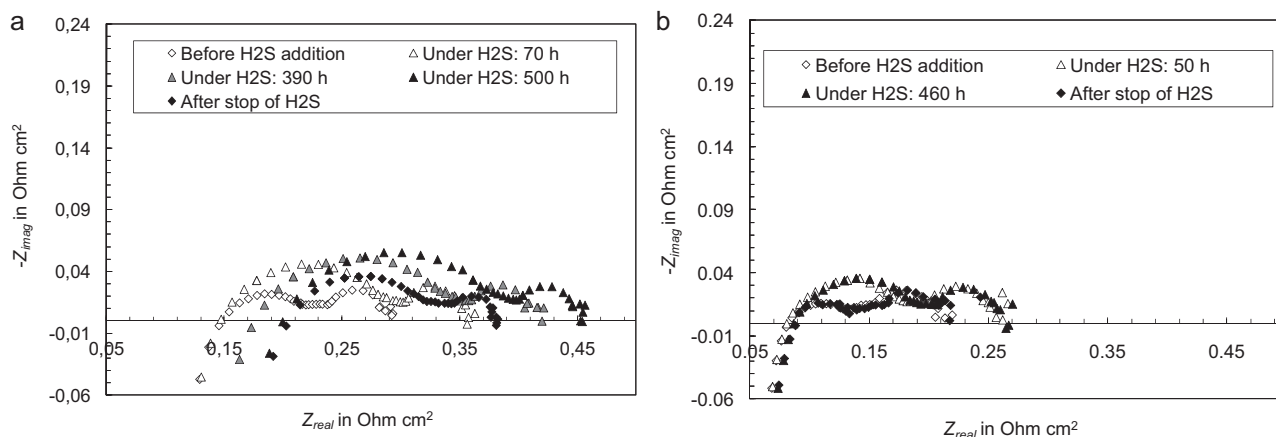
Fig. 4. Selected impedance spectra recorded under current load, at 850 °C, 1 A cm^{-2}, 2 ppm H$_2$S, 13% H$_2$, 58%, H$_2$O 29% CH$_4$ during test of the (a) Ni,YSZ,LSM cell and the (b) Ni,ScYSZ,LSM cell.

sulfur by SO$_2$ and thus mitigate the poisoning effect at higher current loads [20]. The trend of increasing relative cell voltage drop with increasing current density in galvanostatic modes was for example measured by Cheng et al. [21] on electrolyte supported SOFCs. The magnitudes of voltage drops measured here at 0 A cm^{-2} (OCV) were 35 and 24 mV for the Ni,YSZ,LSM and the Ni,ScYSZ,LSM, respectively, and thus smaller than that at 1 A cm^{-2}. These findings seem to contradict each other. However, to correctly evaluate the poisoning effect vs. current density, resistances rather than voltages have to be considered as also put forward by Bøgild Hansen and Rostrup-Nielsen [20] and Cheng et al. [21]. Further, the voltage drops in the current work as seen at OCV and 1 A cm^{-2} cannot be directly compared, because they are due to different effects (gas composition, internal resistance change).

The presented results demonstrate impressively that the cell voltage behaved quite differently over the long-term poisoning for the two cells. In order to obtain more detailed information about the long-term effect of H$_2$S, impedance spectra were recorded under current load. In Fig. 4, selected impedance spectra are shown.

After start of the H$_2$S addition of the fuel, no change of the serial resistance was observed, but the polarization part of the impedance increased on the Ni,YSZ,LSM cell (from white rhombs to white triangles in Fig. 4a). With progressing time under H$_2$S, the spectra gradually shifted towards higher resistances. After stopping the H$_2$S addition, the serial resistance did not change significantly, but the polarization resistance decreased (from black triangles to black rhombs in Fig. 4a).

When starting the H$_2$S addition at the Ni,ScYSZ,LSM cell, the same effects happened: the serial resistance remained constant, while the polarization resistance increased (from white rhombs to white triangles, Fig. 4b). However, the resistance development was very different under H$_2$S exposure. No significant changes were observed; neither on the serial nor polarization resistance, at the time scale of 460 h (compare white and black triangles, Fig. 4b). When stopping the H$_2$S, the impedance spectrum returned to the initial situation (from black triangles to black rhombs, Fig. 4b). Thus, the impedance reflects the same trend as the cell voltages (Fig. 3).

Comparing these results to previous studies on Ni,YSZ,LSM cells [10], the irreversible increase of the serial resistance on this cell type was a new phenomenon. No such increase was observed when the same concentration H$_2$S was added over a period of 24 h [10]. The only difference to this study was the time scale, i.e. a longer exposure to H$_2$S than 24 h is necessary to induce the effect on the serial resistance.

To obtain more time resolved information about the processes under H$_2$S exposure, all the serial (*Rs*) and polarization (*Rp)* resis-

tance values derived from the impedance spectra recorded under current load are plotted for the Ni,YSZ,LSM cell in Fig. 5 and for the Ni,ScYSZ,LSM cell in Fig. 6.

Two distinct regions of different resistance trends, and thus probably also degradation mechanisms, can be identified for the Ni,YSZ,LSM cell (see Fig. 5). Initially, *Rs* did not change significantly (only slight increase after ∼50 h). On the other hand, *Rp* increased tremendously. This observation confirms results of the mentioned previous studies, where the H$_2$S exposure was limited to 24 h [10]. Afterwards, the polarization resistance increased to a smaller extent than *Rs*. Here an increase by ∼50% occurred. When stopping the H$_2$S flow, *Rp* decreased immediately, i.e. the effect of H$_2$S on *Rp* was reversible to a large degree, which was also found in the studies with 24 h exposure to H$_2$S [10]. *Rs* on the other hand did not decrease when H$_2$S was stopped. On the contrary, it even continued to increase, however, with a significantly smaller rate than under H$_2$S exposure. The effect of H$_2$S on *Rs* was thus irreversible. A simple covering of the anode surface by H$_2$S is thus not very probable as the exclusive origin of the degradation under H$_2$S. Such a cover layer would be gradually removed when H$_2$S is stopped [6,10].

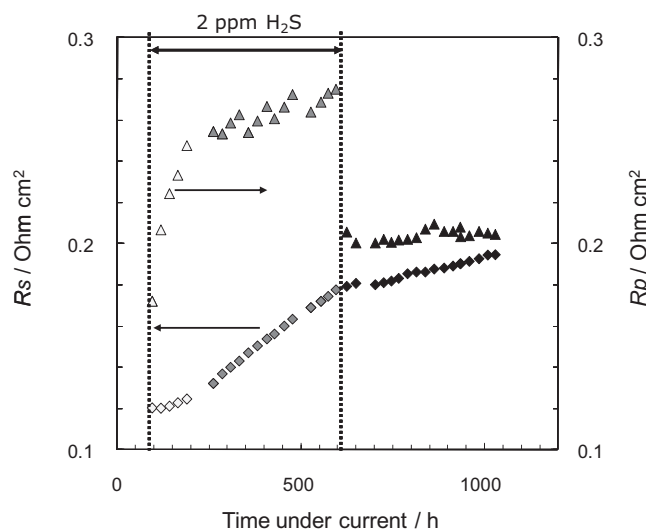**Fig. 5.** Ni,YSZ,LSM cell, *Rs* (rhombs) and *Rp* (triangles) derived from impedance spectra recorded under current load, at 850 °C, 1 A cm^{-2}, 2 ppm H$_2$S, 13% H$_2$, 58%, H$_2$O 29% CH$_4$.
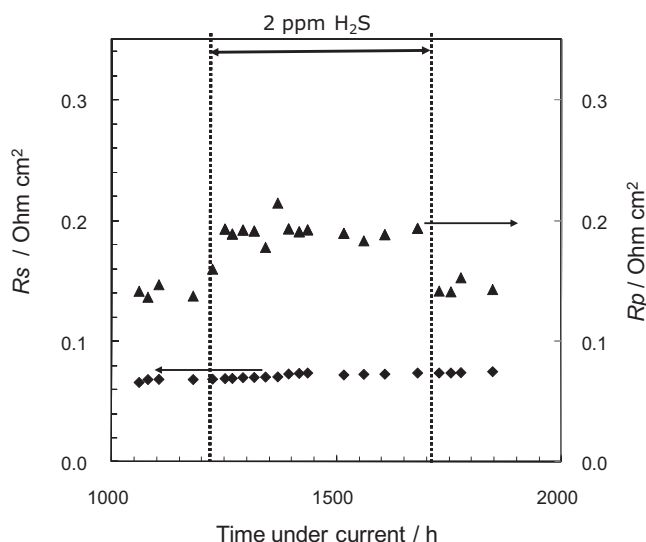
Fig. 6. Ni,ScYSZ,LSM cell, Rs (rhombs) and Rp (triangles) derived from impedance spectra recorded under current load, at 850 °C, 1 A cm^{-2}, 2 ppm H$_2$S, 13% H$_2$, 58%, H$_2$O 29% CH$_4$.

On the Ni,ScYSZ,LSM cell, Rs did not change significantly, neither when starting the H$_2$S addition nor during long term exposure (see Fig. 6). Rp, on the other hand, increased rapidly (and reversibly) when starting (and stopping) the H$_2$S addition to the fuel, while it remained nearly constant during the H$_2$S exposure. These results are in line with the observed cell voltage trends (see Fig. 3).

A common feature for both cells is that Rp increased initially under H$_2$S exposure. A quantitative analysis showed the increase to be ~48% for the Ni,YSZ,LSM cell and ~40% for the Ni,ScYSZ,LSM cell. These trends are not too different from each other. The smaller resistance change on the Ni,ScYSZ,LSM cell could be related to the lower overall resistance of this cell. As already shown for the OCV case (see Section 3.1 and Fig. 2), the reforming activity was obviously poisoned to similar degrees on both cell types. It is thus tempting to relate the increase of Rp when starting H$_2$S exposure under current in both cases to a coverage of the active sites (three phase boundary) by sulfur.

However, the irreversible increase of Rs during the long-term exposure towards H$_2$S occurred only on the Ni/YSZ/LSM cell. A microstructural analysis of the cell was carried out in order to see whether the changes of the electrochemical properties can be related to microstructural characteristics (see Section 3.3).

As the Ni,ScYSZ,LSM cell showed a considerable tolerance towards 2 ppm H$_2$S, it was interesting to study the effect of current load and higher H$_2$S concentrations.

Current load was expected to improve the tolerance towards H$_2$S, as oxygen ions transferred through the electrolyte during operation under current load could oxidize adsorbed sulfur species [8,15,21–24]. A long-term test was run at OCV and 850 °C in the presence of 2 ppm H$_2$S over 500 h. The cell voltage degradation rate was 3 mV kh^{-1} (0.3%) on the Ni,ScYSZ,LSM cell. This value was thus not significantly larger than the one under 1 A cm^{-2} (zero mV kh^{-1}). Either, current load has no significant effect or the effect is not visible because the cell was operated in a safe regime with regards to the H$_2$S poisoning. It has also to be taken into consideration that the poisoning of the electrochemical oxidation of hydrogen is contributing under current load.

In order to evaluate the tolerance of the cell towards larger H$_2$S concentrations, durability tests over 200 h were performed using the same H$_2$/CH$_4$/H$_2$O fuel mixture as before with 10 and 20 ppm H$_2$S, at 850 °C and 0.44 A cm^{-2} (Fig. 7). The cell voltage degradation rates were 68 mV kh^{-1} (6%) and 156 mV kh^{-1} (8%) for 10 and
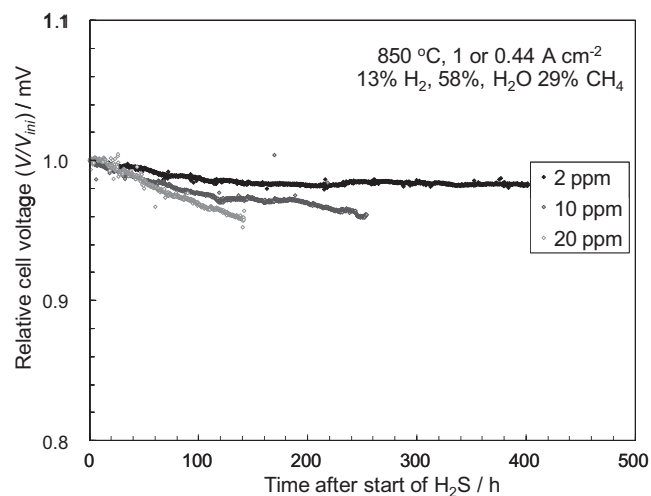

Fig. 7. Cell voltage (relative values) on the Ni,ScYSZ,LSM cell in a 13% H$_2$, 58%, H$_2$O 29% CH$_4$ fuel at 850 °C, under 2 ppm H$_2$S (1 A cm^{-2}), 10 and 20 ppm (0.44 A cm^{-2}).

20 ppm H$_2$S, respectively. This is a first indication that a poisoning effect started to occur at these larger H$_2$S concentrations, however, with the restriction that these tests were performed at a lower current density than the test under 2 ppm H$_2$S.

3.3. Microstructural analysis after long-term testing under H$_2$S

The two cells were studied by SEM after long-term testing, the Ni,YSZ,LSM cell after an operation period of 1500 h in total, and the Ni,ScYSZ,LSM after even longer testing and more sulfur exposure periods; the total testing time was 10,500 h for this cell. A first evaluation of the Ni particle sizes and distributions did not reveal significant differences. However, when focusing on the percolation of Ni particles, significant differences became visible. Fig. 8 shows the cross section of the electrolyte/anode interfaces taken at low accelerating voltage mode, where the percolating Ni particles appear as light spots.

In the Ni,YSZ,LSM cell, the anode particles within the first few μm from the electrolyte appear dark, i.e., they are not percolat-
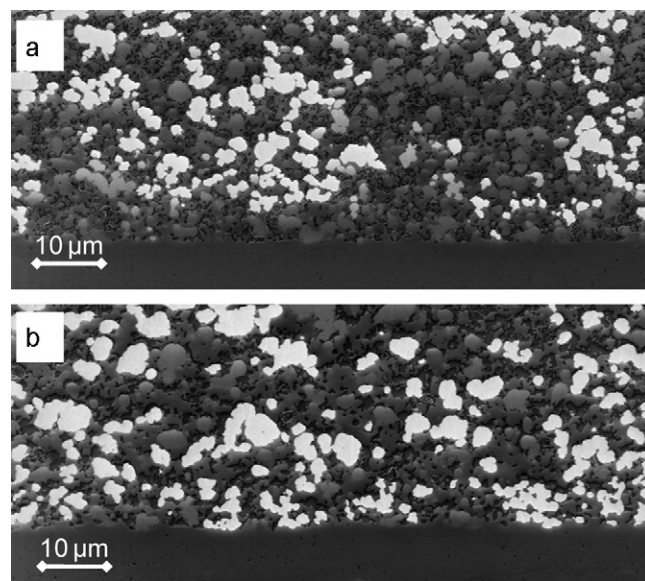

Fig. 8. Polished cross sections of the electrolyte/anode interface of the tested Ni,YSZ,LSM (a) and Ni,ScYSZ,LSM (b) cells, the lower dark layers are the electrolytes, light spots are percolating Ni particles in the anode and anode support.

ing any more after testing (Fig. 8a). This finding would explain the observed irreversible increase of the serial resistance (see Fig. 5). The process is slow and becomes first visible by an increase of the serial resistance after 50–100 h exposure to H_2S. It is therefore also distinctly different from the coverage of active sites by sulfur, which is fast and reversible and only affecting the polarization resistance. Further, a loss of percolation does not necessarily need to be accompanied by extensive changes of the particle size distribution, which explains the lack of evidence for significant coarsening in the anodes of the two tested SOFCs.

In contrast, in the Ni,ScYSZ,LSM cell, light spots are visible over the whole shown cross section, also close to the electrolyte (Fig. 8b). The percolation of Ni is therefore still intact over the whole anode cross section, in particular close to the electrolyte. These results suggest that H_2S in combination with high polarization promotes the loss of percolation of the Ni-particles close to the electrolyte. In that case, the magnitude of anode polarization would be an important factor and explain the better intactness of the percolated Ni-network (H_2S tolerance) of the Ni, ScYSZ,LSM cell.

The SEM studies also demonstrate how important the development and application of appropriate, advanced imaging techniques are, when aiming at the identification of structural origins of observed cell voltage degradation processes.

4. Conclusions

Summarizing, a similar immediate cell voltage drop was observed for the first time on anode supported Ni,YSZ,LSM and Ni,ScYSZ,LSM cells (the Ni,ScYSZ,LSM cell maybe to a smaller extent) when exposed to H_2S concentrations between 2 and 24 ppm at OCV and 850 °C in a fuel consisting of 13% H_2, 29% CH_4, and 58% H_2O. This cell voltage drop was due to the gradual poisoning of the methane reforming reaction, which obviously occurred to a similar extent on both SOFC types.

When operating at $1 A cm^{-2}$ current load in the presence of 2 ppm H_2S over 500 h, the cell voltage of the Ni,YSZ,LSM cell degraded significantly, mainly due to an irreversible increase of the serial resistance, which was observed using impedance spectroscopy under current load. Micro-structural analysis revealed that this increase is due to a loss of percolation of the Ni particles in the layers closest to the electrolyte, while the particle size distributions did not change to a large extent. Such a long-term effect of the presence of as small amounts of H_2S as 2 ppm at 850 °C has not been reported before.

A Ni,ScYSZ,LSM cell did not show any cell voltage degradation under these conditions when considering the final 300 h operating under H_2S exposure. Only when increasing the H_2S concentrations to 10 and 20 ppm, a cell voltage degradation was observed. The effect of current load vs. OCV on the tolerance of the Ni,ScYSZ,LSM cell towards H_2S was not significant under the operating conditions in this study.

Acknowledgements

References

[1] H. Yokokawa, T. Hengyong, B. Iwanschitz, A. Mai, J. Power Sources 182 (2008) 400–412.
[2] A. Hagen, R. Barfod, P.V. Hendriksen, Y.-L. Liu, S. Ramousse, J. Electrochem. Soc. 153 (2006) A1165–A1171.
[3] M. Mogensen, K. Kammer, Annu. Rev. Mater. Res., 33 (2003) 321.
[4] J.R. Rostrup-Nielsen, J. Sehested, J.K. Nørskov, Adv. Catal. 47 (2002) 65.
[5] K. Sasaki, K. Susuki, A. Iyoshi, M. Uchimura, N. Imamura, H. Kusaba, Y. Teraoka, H. Fuchino, K. Tsujimoto, Y. Uchida, N. Jingo, J. Electrochem. Soc. 153 (2006) A2023–A2029.
[6] J.F.B. Rasmussen, A. Hagen, J. Power Sources 191 (2009) 534–541.
[7] S. Zha, Z. Cheng, M. Liu, J. Electrochem. Soc. 154 (2007) B201–B206.
[8] J.R. Rostrup-Nielsen, J.B. Hansen, S. Helveg, N. Christiansen, A.K. Jannasch, Appl. Phys. 85 (2006) 427.
[9] M. Noponen, M. Halinen, J. Kiviaho, J. Saarinen, J. Fuel Cell Sci. Technol. 3 (2006) 438–444.
[10] J.F.B. Rasmussen, A. Hagen, Fuel Cells 10 (2010) 1135–1142.
[11] M. Smith, A.J. McEvoy, Proc. 7th European Solid Oxide Fuel Cell Forum, Lucerne 3–7. July 2006.
[12] M. Smith, A.J. McEvoy, ECS Transactions – Solid Oxide Fuel Cells vol. 7, June 2007 for 10th International Symposium on Solid Oxide Fuel Cells (SOFC-X), Nara, Japan, 2007, pp. 373.
[13] A. Hagen, M. Menon, S. Ramousse, P.H. Larsen, R. Barfod, P.V. Hendriksen, Fuel Cells 6 (2006) 146–150.
[14] T. Ramos, J. Hjelm, M. Wandel, A. Hagen, M. Mogensen, ECS Transact. 13 (2008) 235.
[15] M. Mogensen, P.V. Hendriksen, High temperature solid oxide fuel cells, in: S.C. Singhal, K. Kendall (Eds.), Fundamentals, Design, and Applications, Elsevier, 2003, chapter 10.
[16] K. Thydén, Y.L. Liu, J.B. Bilde-Sørensen, Solid State Ionics 178 (2008) 1984.
[17] Y. Lin, Z. Zhan, J. Liu, S.A. Barnett, Solid State Ionics 176 (2005) 1827.
[18] K. Sasaki, K. Susuki, A. Iyoshi, M. Uchimura, N. Imamura, H. Kusaba, Y. Teraoka, H. Fuchino, K. Tsujimoto, Y. Uchida, N. Jingo, Sulfur Tolerance of Solid Oxide Fuel Cells, Proc. SOFC IX, 1267–1274.
[19] K. Eguchi, K. Tanaka, T. Matsui, R. Kikuchi, Catal. Today 146 (2009) 154–159.
[20] J. Bøgild Hansen, J. Rostrup-Nielsen, Chapter 65: Sulfur poisoning on Ni catalyst and anodes, in: W. Vielstich, H. Yokokawa, H.A. Gasteiger (Eds.), Handbook of Fuel Cells–Fundamentals, Technology and Applications, vol. 6, John Wiley & Sons, 2009.
[21] Z. Cheng, S. Zha, M. Liu, J. Power Sources 172 (2007) 688.
[22] J.H. Koh, Y.-S. Yoo, J.-W. Park, H.C. Lim, Solid State Ionics 149 (2002) 157.
[23] T. Horita, K. Yamaji, T. Kato, H. Kishimoto, Y. Xiong, N. Sakai, M.E. Brito, H. Yokokawa, J. Power Sources 145 (2005) 133.
[24] Z. Zhang, Y. Lin, M. Pillai, I. Kim, S.A. Barnett, J. Power Sources 161 (2006) 460–465.